minerals

MDPI

Article

A Study of Shock-Metamorphic Features of Feldspars from the Xiuyan Impact Crater

Feng Yin * and Deqiu Dai

Hunan Provincial Key Laboratory of Shale Gas Resource Utilization, Hunan University of Science and Technology, Xiangtan 411201, China; ddqygf@163.com

* Correspondence: yinfeng@hnust.cn

Received: 17 January 2020; Accepted: 2 March 2020; Published: 3 March 2020

Abstract: Feldspar is the most abundant mineral in the Earth's crust and is widely distributed in rocks. It is also one of the most common minerals in meteorites. Shock-metamorphic features in feldspar are widely used to calibrate the temperature and pressure of shock events and can also provide clues for searching for impact craters on Earth. In this study, shocked alkali feldspars in the lithic breccia and suevite from Xiuyan Impact Crater were investigated using polarizing optical microscopes, Raman spectroscopy and electron microprobes to better constrain the shock history of this crater. For this study, feldspar grains occurring in gneiss clasts in the impact breccia and four shock stages were identified, e.g., weakly shocked feldspar, moderately shocked feldspar, strongly shocked feldspar, and whole rock melting. According to the shock classification system for alkali feldspar and felsic rocks, we estimated the shock pressure (SP) and post-shock temperature (PST) histories of these gneiss clasts. Weakly shocked feldspars display irregular fractures and undulatory extinction, and their shock stage is F-S2, which indicates that SP and PST are from ~5 to ~14 GPa and ~100 °C, respectively. Moderately shocked feldspars show planar deformation features and are partially transformed into diaplectic glass, which indicates that the F-S5 shock stage of SP and PST is from ~32 to ~45 GPa and 300–900 °C. Strongly shocked feldspars that occur as vesicular glass indicate a shock stage of F-S6, and the SP and PST are 45–60 GPa and 900–1500 °C, respectively. The whole felsic rock melting occurs as mixed melt glass clast and belongs to the F-S7 stage, and SP and PST are >60 GPa and >1500 °C, respectively.

Keywords: feldspar; shock-metamorphic features; high pressure and high temperature; Xiuyan Impact Crater

1. Introduction

Feldspar, a framework silicate, is a common rock-forming mineral that is widely distributed in igneous, metamorphic and sedimentary rocks [1]. Feldspar is also the most abundant mineral in the Earth's crust, accounting for about 50% of the total weight of the Earth's crust [1]. In addition, feldspar is also a common mineral in ordinary chondrites and in meteorites from Mars, the Moon and Vesta [2]. The high temperature and high pressure induced by an impact event can cause special deformation features in rocks and minerals, known as shock metamorphism [3]. Shock features of feldspar have been observed in impactites from impact craters on Earth [4,5], ordinary chondrites [6,7], as well as Vesta [8], Lunar [9] and Martian [10] meteorites. The currently known shock-metamorphic features in natural feldspar include irregular fractures and planar fractures [5], undulatory extinction and mosaicism [11], planar deformation features (PDFs) [12], diaplectic glass (sometimes called maskelynite) [4,13], vesicular glass [14], lingunite [15], and decomposition [16]. The shock-metamorphic features of feldspar can provide clues for the search for impact craters on Earth and can also enrich the understanding of the behavior of feldspar under high temperatures and high pressures.

The Xiuyan crater is a simple impact crater located in northeast China with a diameter of 1800 m, which was formed 50,000 years ago [17]. The basement rocks in the impact crater area are crystalline rocks composed of gneiss, granulite, and amphibolite, as well as minor basalt and marble. A drill hole at the center of the Xiuyan crater reveals that the crater contains a loosely consolidated impact breccia lens with a center thickness of about 188 m, which is underlain by 107-m-thick lacustrine sediments [17]. The upper part of the 153 m thick part of the impact breccia lens consists of gneiss, amphibolite, basalt, and marble fragments as well as a small amount of lithic breccia, whereas the lower 35 m thick part of the impact breccia lens is composed of gneiss, granulite and amphibolite fragments and small amount of melt-bearing breccia (suevite).

So far, a variety of high-pressure minerals have been found in the suevite from the Xiuyan crater, such as coesite [14], reidite [18], TiO_2-II [19], diamond [20], and maohokite [21]. This study focuses on the shock-metamorphic features of feldspar in impact breccias from the Xiuyan crater, and we try to reveal the shock histories of these feldspars.

2. Sample and Methods

The two hand samples used for this study were impact breccias. One was a lithic breccia that was recovered from the drill hole at a depth of 135 m and the other was a suevite that was recovered from the drill hole at a depth of 260–295 m. Initial examination of the polished thin sections with an optical microscope under transmitted and reflected light confirmed the shock stages of feldspar grains. Raman spectroscopy and electron probe microanalysis (EPMA) were done at the Guangzhou Institute of Geochemistry, Chinese Academy of Science (Guangzhou, China) in order to identify the minerals and measure their chemical compositions. Raman spectra of minerals were measured in the range of 200–1200 cm^{-1} by a Renishaw RM-2000 instrument (Ar^+ laser, 514 nm line, 2 μm wide spots) with a 20 s acquisition time and a power level of 20 mW. Backscattered electron (BSE) images and quantitative analyses of minerals were done using a JEOL JXA-8100 EPMA. The analyses were conducted with an acceleration voltage of 15 kV, a beam current of 10 nA, a beam diameter of 1 μm, and a peak counting time of 10–20 s. The quantitative data obtained were in weight percentage of oxides (wt%). The standards used were albite (Si, Al and Na), anorthosite (Ca), potassium feldspar (K), garnet (Fe) and TiO_2 (Ti). Analytical results were reduced using a ZAF correction program.

3. Results

3.1. Petrology of Impact Breccias

Both lithic breccia and suevite are polymict breccia. Lithic breccia consists of a matrix and clasts (Figure 1a). The clasts account for about 70% of the whole breccia and are composed of a variety of different rocks and minerals, including basalt, amphibolite and gneiss as well as quartz, feldspar, pyroxene and amphibole. The matrix, accounting for about 30% of the whole breccia, is mainly composed of fine-grained quartz and feldspar. The suevite consists of clasts, a matrix, and glass clasts (Figure 1b). The clasts account for about 40% of the whole breccia and consist of rocks and minerals, including gneiss, amphibolite, quartz and feldspar. The matrix accounts for about 50% of the whole rock, including quartz, feldspar, amphibole, calcite, zircon and magnetite as well as microcrystalline materials. The glass clasts account for 5–10% of the whole breccia and are irregularly shaped, ranging from a few microns to nearly millimeters.

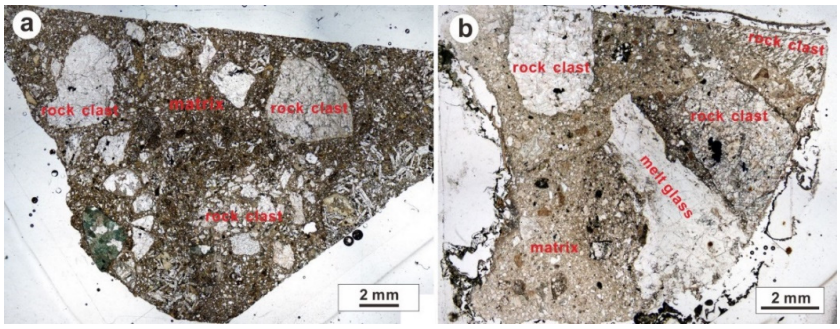

Figure 1. Mosaic images of thin sections of the lithic breccia (**a**) and suevite (**b**) (plane polarized light, PPL).

In general, feldspar grains are the main components of both the two impact breccias, and they are widely distributed in the matrix and clasts of the impact breccias. Our study focused on the feldspars in the rock clasts in the impact breccias. According to the shock-metamorphic features developed in feldspar grains, these feldspars are divided into four categories: weakly shocked feldspar, moderately shocked feldspar, strongly shocked feldspar, and whole rock melting.

3.2. Weakly Shocked Feldspar

Weakly shocked feldspar grains can be found in both lithic breccia and suevite. The shape of weakly shocked feldspar is well preserved, but most of them contain irregular fractures (Figure 2). Under cross-polarized light, they show optical interference color of first-order gray, and some feldspars display undulatory extinction (Figure 2d). The Raman spectrum shows that weakly shocked feldspar has peaks at 291, 480, 509, 640, 816, 1114, and 1186 cm^{-1} (Figure 3), and there is no significant difference compared with the unshocked feldspar, except for a lack of peaks at 210 and 765 cm^{-1}. The chemical compositions of weakly shocked feldspars show there are two kinds of feldspar. One mainly contains 64.5–68.9 wt% SiO_2, 18.48 wt% Al_2O_3, 0.45 wt% Na_2O and 16.32 wt% K_2O (Table 1) and can be classified as orthoclase (Figure 4). The other mainly contains 68.9 wt% SiO_2, 19.62 wt% Al_2O_3, 8.61 wt% Na_2O and 1.15 wt% K_2O (Table 1) and can be classified as albite (Figure 4).

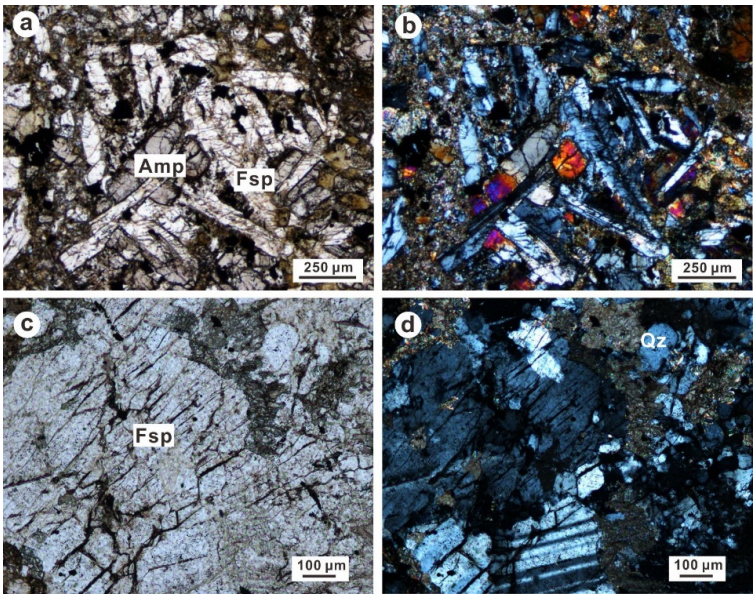

Figure 2. Weakly shocked feldspars. (**a**) Feldspar grains in lithic breccia display irregular fractures (PPL). (**b**) Some feldspar grains show undulatory extinction (cross polarized light, XPL). (**c**,**d**) Feldspar grains in suevite display many irregular fractures and undulatory extinction (c—PPL, d—XPL). Fsp—Feldspar, Amp—Amphibole, Qz—Quartz.

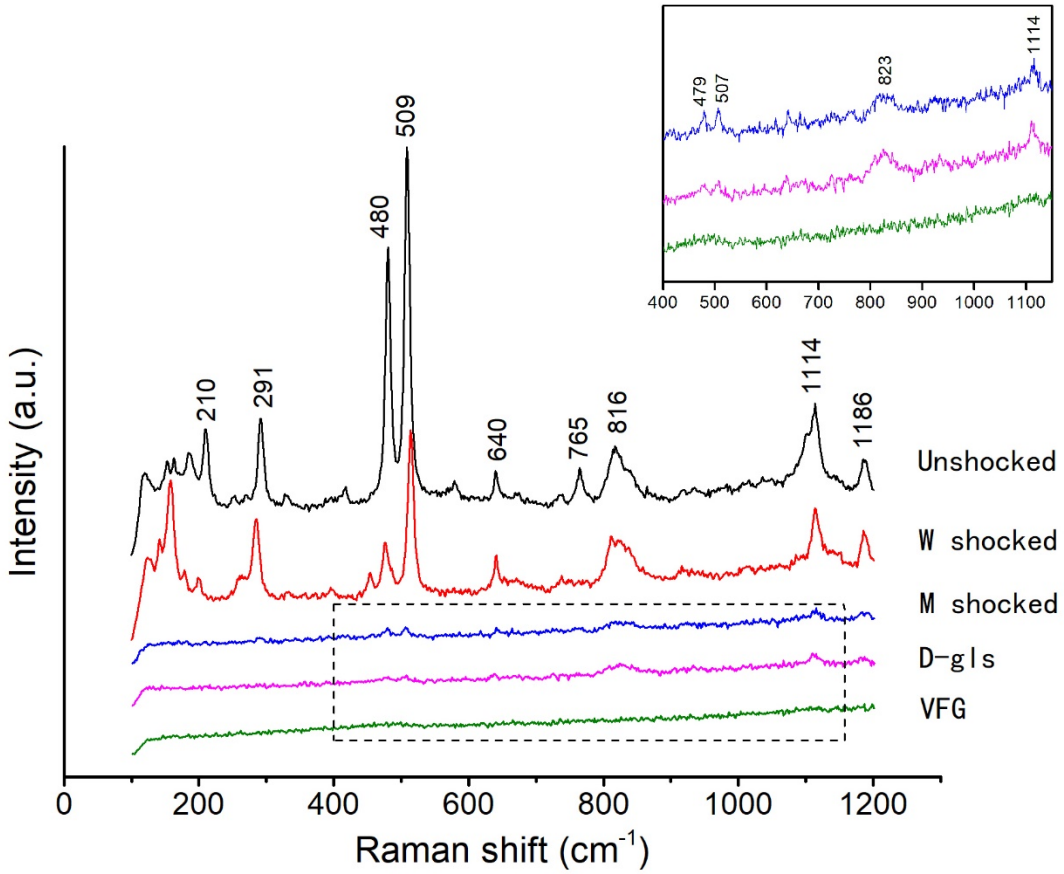

Figure 3. Representative Raman spectra of shocked feldspars. From top to bottom: unshocked feldspar (Unshocked), weakly shocked feldspar (W shocked), moderately shocked feldspar (M shocked), diaplectic feldspar glass (D-gls) and vesicular feldspar glass (VFG). The inset represents the area indicated by dashed box.

Table 1. Representative contents of major elements (wt%) in weakly shocked feldspars, moderately shocked feldspars and melt glasses.

Oxide (wt%)	Weakly Shocked		Moderately Shocked		Melt Glasses			
			D-gls	Crystalline	VFG		MMG	
SiO_2	64.53	68.90	71.03	69.88	75.33	66.46	69.17	55.15
TiO_2	-	0.00	0.01	-	-	0.03	0.47	0.64
Al_2O_3	18.48	19.62	19.47	19.22	18.41	19.74	13.90	19.75
FeO	0.08	0.05	0.06	0.12	0.12	0.68	5.25	7.60
MnO	0.04	-	0.00	0.02	0.03	0.01	0.07	0.18
MgO	0.01	0.01	0.01	0.00	0.01	0.09	1.88	4.18
CaO	0.00	0.32	0.17	0.25	0.14	0.96	2.55	6.39
Na_2O	0.45	8.61	8.09	8.78	1.10	6.60	1.22	0.19
K_2O	16.32	1.15	0.43	0.36	0.83	0.56	2.20	3.50
P_2O_5	-	0.00	0.02	0.02	-	0.01	0.04	0.03
Total	99.91	98.66	99.29	98.65	95.98	95.14	96.75	97.60
An	0.0	3.6	2.2	3.0	8.6	13.2		
Ab	4.0	88.6	94.5	94.5	61.0	82.2		
Or	96.0	7.8	3.3	2.6	30.4	4.6		

D-gls—diaplectic feldspar glass, VFG—vesicular feldspar glass, MMG—mixed melt glass.

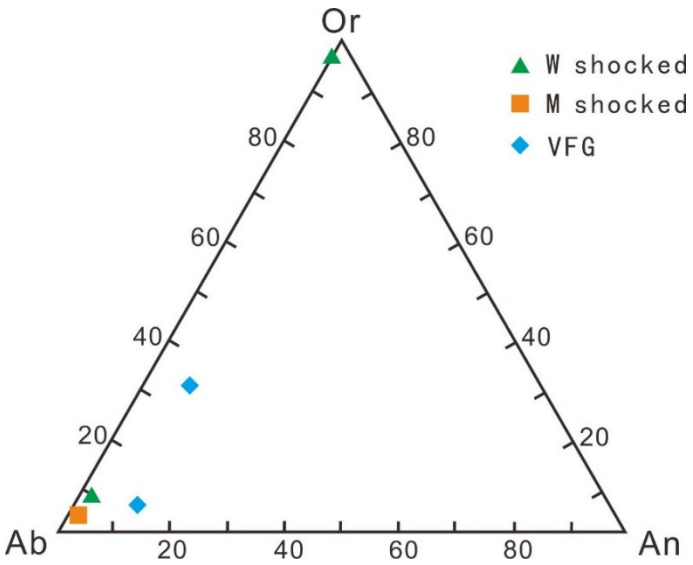

Figure 4. Ternary diagram for feldspars. Green symbol—weakly shocked feldspar (W shocked), Yellow symbol—moderately shocked feldspar (M shocked), Blue symbol—vesicular feldspar glass (VFG). Ab—albite, An—anorthite, Or—orthoclase.

3.3. Moderately Shocked Feldspar

Moderately shocked feldspars were observed in some gneiss fragments from suevite. In these rock fragments, feldspars keep their original shape but show abnormal optical properties. Figure 5a,b shows a partial vitrified feldspar grain. Under cross-polarized light, the optical interference color is first-order gray, which is slightly reduced compared with the normal interference color, and some parts of the feldspar remain extinct on rotation of the stage, indicating that they have become isotropic. Figure 5c,d shows a distinctive ladder structure that alternates twin lamellae of a feldspar grain that have either been transformed into diaplectic glass or are crosscut by short, closely spaced PDFs. PDFs generally have only one set with a width of <1 μm and a spacing of 2–4 μm (Figure 5c). The apparent angles between the PDFs and the twin lamellae are 30°–90°. A similar shock induced ladder structure in feldspar from the Ries crater was also observed by Stöffler [4]. On the BSE image, the brightness of the diaplectic glass is lower than that of the crystalline part of the feldspar, and the boundaries between them are clear and sharp (Figure 5d).

The crystalline part of the feldspar has Raman peaks of 479, 507, 823, and 1114 cm^{-1}, but the intensity is very weak (Figure 3), whereas the Raman spectrum of the diaplectic feldspar glass part only shows peaks at 823 and 1114 cm^{-1} (Figure 3). The chemical compositions of the crystalline part and diaplectic glass part are similar. They mainly contain 69.88–71.03 wt% SiO_2, 19.22–19.47 wt% Al_2O_3, 0.17–0.25 wt% CaO, 8.09–8.61 wt% Na_2O and 0.36–0.43 wt% K_2O (Table 1) and can be classified as albite (Figure 4). The EPMA and Raman spectra from the diaplectic glass and crystalline feldspar are mixed signals due to the narrow spacing between diaplectic glass and crystalline feldspar (Figure 5d).

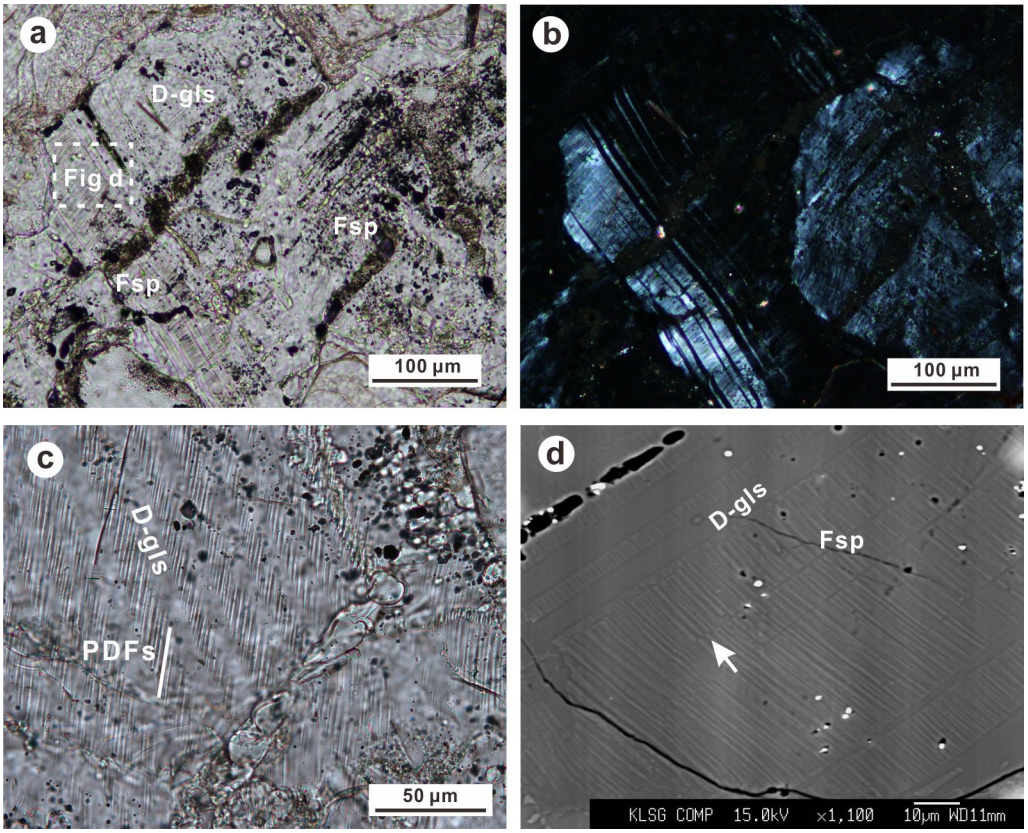

Figure 5. Moderately shocked feldspars. (**a**,**b**) Feldspar grains show an interference color of first order gray and are partially transformed into glass (a—PPL, b—XPL). (**c**) A feldspar grain shows one set of PDFs and diaplectic glass (PPL). (**d**) BSE image of the twin lamellae that have been converted to diaplectic glass. Fsp—Feldspar, D-gls—Diaplectic feldspar glass.

3.4. Strongly Shocked Feldspar

Strongly shocked feldspar grains are found in the gneiss fragments from the suevite and are completely transformed into vesicular feldspar glass (VFG). VFG does not show a flow texture and contains abundant of vesicles with diameters ranging from 5 to 20 μm (Figure 6a,b). The vesicles take up 40% of the glass by volume. VFG always coexists with coesite-bearing silica glass. There are clear boundaries between VFG and silica glass, indicating they do not mix with each other (Figure 6c). No peaks can be identified from the Raman spectrum of the VFG (Figure 3). EPMA shows that the chemical compositions of VFGs are similar to albite and anorthoclase (Table 1 and Figure 4). The total chemical compositions of vesicular albite glass are only 95.98% and 95.14% due to the 1 μm beam of EPMA.

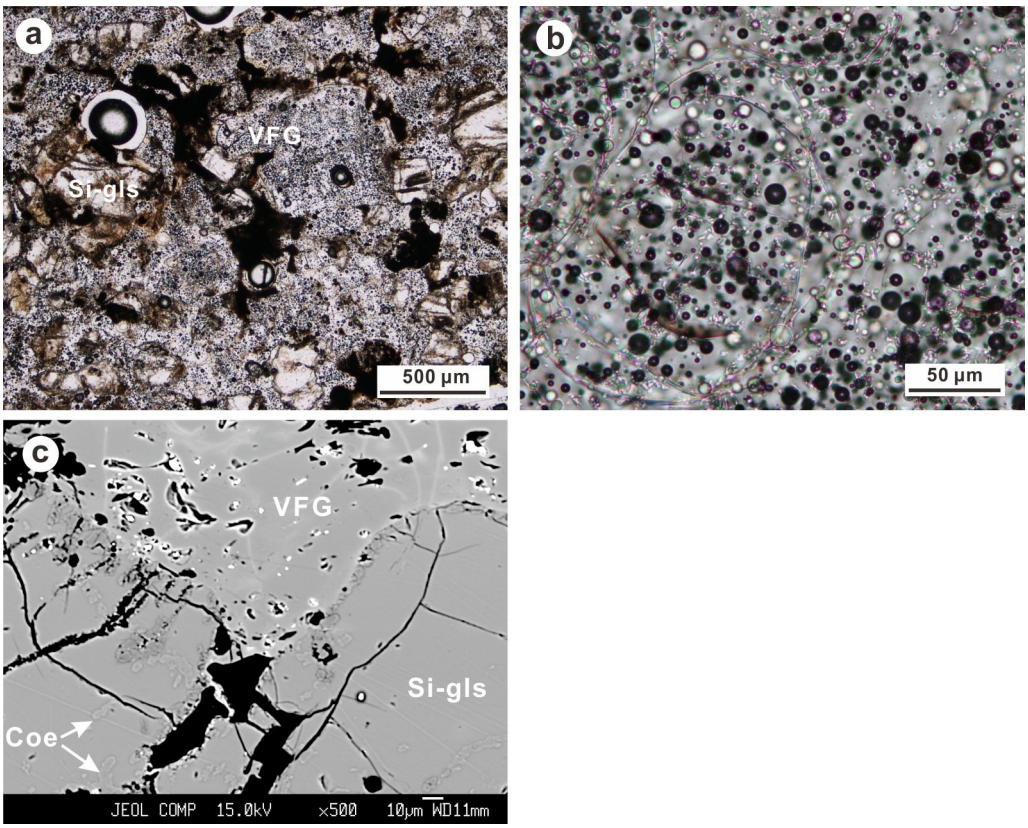

Figure 6. Strongly shocked feldspars. (**a**,**b**) VFG contains abundant vesicles (PPL). (**c**) BSE image shows that VFG coexists with coesite-bearing silica glass and the boundary between them is clear. Si-gls—Silica glass, Coe—Coesite.

3.5. Mixed Melt Glass

Mixed melt glass (MMG) clasts are observed in the suevite and occur as irregular patches with sizes of up to 2 mm × 6 mm (Figures 1b and 7a). Most of the MMGs show obvious flow texture. The BSE image of MMG shows clear streaks and many irregular cracks in the glass (Figure 7b). Chemical compositions of MMG have higher contents of FeO (5.25–7.6 wt%) and MgO (1.88–4.18 wt%) than VFG (Table 1), indicating the MMG is a mixture of felsic and mafic minerals. MMG is transparent under plane-polarized light and extinct on rotation under crossed-polarized light, indicating it is an isotropic material (Figure 7c,d). MMG always contains mineral clasts such as quartz, feldspar, zircon and magnesite.

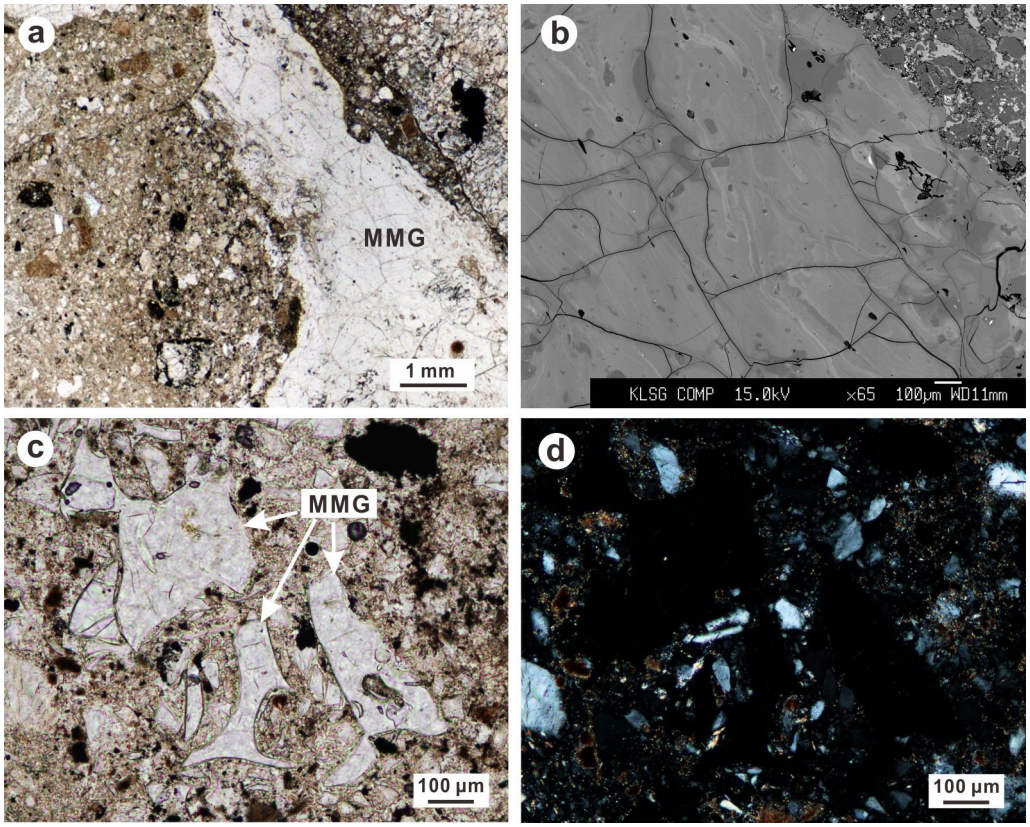

Figure 7. (**a**) A large MMG in the suevite (PPL). (**b**) BSE image of MMG shows schlieren and irregular fractures. (**c**,**d**) Some small MMGs have irregular shapes and are extinct under XPL.

4. Discussion

4.1. Estimation of Shock Pressure

The shock pressure history of minerals can be constrained according to the shock-metamorphic features. However, shock pressure can be extremely local and heterogeneous, and depends on a wide range of things (temperature of target, water content, strain rate, porosity, etc.) [22–26]. Therefore, we can only get rough shock pressures of natural shock events according to shock features in minerals. In this study, the lithic breccias and suevites are polymict breccias that consist of multiple lithology targets of different shock levels. So, the shock pressure of feldspars in the gneiss clasts are only for the gneiss fragments and not for the whole impact breccias. To estimate the shock pressure history of shocked feldspar, we must consider its chemical composition (i.e., relative proportions of Ca, Na, and K), because the formation pressure of shock features in feldspar is closely related to its chemical composition. A study on maskelynite by Rubin [27] showed that the formation pressure of maskelynite is ~20–30 GPa, depending on the Ca concentration. Stöffler et al. [11] summarized shock-metamorphic effects from both impact craters and meteorites and indicated that the pressure that is required to form PDFs and diaplectic glass in alkali feldspar is higher than that of plagioclase. In this study, feldspars were all identified as alkali feldspar (Figure 4) and were always distributed in gneiss clasts in the lithic breccia and suevite. Therefore, the latest shock classification system for alkali feldspar and felsic rocks by Stöffler et al. [11] could be used to estimate shock pressures in this study.

Weakly shocked alkali feldspar mainly developed irregular fractures and undulatory extinction, and the shock pressure was estimated to be ~5 to ~14 GPa. Moderately shocked alkali feldspar has both PDFs (~10–34 GPa) and diaplectic glass (~32–45 GPa), indicating pressures of ~32 to ~45 GPa. Strongly shocked vesicular alkali feldspar glass indicates a shock pressure of 45–60 GPa. MMG shows

a schlieren texture, indicating it mixes incompletely with the other melt before cooling. Therefore, MMG represents whole rock melts, which indicates a shock pressure of >60 GPa.

4.2. Diaplectic Feldspar Glass or Maskelynite?

Maskelynite, a common phase in shocked meteorites, is an amorphous phase of plagioclase composition. The term maskeynite was first proposed by Tschermak [28] to describe the labradorite glass of unknown origin in the Martian Shergotty meteorite. The term diaplectic glass was first proposed by Von Engelhardt et al. [13] to describe quartz or feldspar glass formed by solid-state phase transformation in suevites from the Ries crater, Germany. Maskelynite is generally thought to be formed by shock-induced solid-state transformation of feldspar that does not undergo a melting process [27]. Therefore, many researchers regard the two terms as the same kind of phase, i.e., maskelynite is equivalent to diaplectic feldspar glass. However, Chen et al. [29] studied maskelynite from L-chondrites and Martian meteorites, arguing that maskelynite is not diaplectic glass, but a dense quenched glass formed by shock-induced melting and quenching. Chen et al.'s [29] research showed that maskelynite does not contain fractures or cleavage, displays radiating cracks, and is enriched in potassium. In view of the controversy over the origin of maskelynite, we prefer to use the term diaplectic feldspar glass rather than maskelynite in this study. The moderately shocked feldspar in this study shows that alternate twin lamellae were converted to diaplectic glass without flow texture or chemical composition changes, which is consistent with the characteristics of solid-state phase transformation. Diaplectic feldspar glass formation in alternate twin lamellae has been reported previously in Ries crater [4], Vredefort [30] and Mistastin Lake impact structures [5], and was explained to be a result of an unsymmetrical orientation of the twinning-plane to the normal of the shock front [4,5].

4.3. Raman Spectrum of Shocked Feldspars

Raman spectra can be used to study the progressive and systematic changes in the crystal lattice structures of naturally shocked feldspars affected by shock wave [5]. Raman spectral peaks at 400–550 cm^{-1} and 900–1200 cm^{-1} indicate changes in silica tetrahedra and within silica tetrahedra [31,32]. Raman spectra of shocked feldspar show broadening and loss of peaks with increasing pressure [12,24,31–33]. In this study, the Raman peaks at 400–550 cm^{-1} and 900–1200 cm^{-1} of weakly shocked feldspar were similar to those of unshocked feldspar, but there was a little broadening at 480 cm^{-1} (Figure 3), which is consistent with the low-level deformation of feldspars from the Tenoumer impact structure [12] and the Lake Mistastin crater [5]. The shock experiment conducted by Kayama et al. [33] on sanidine also confirmed that a shock pressure of 10 GPa would not affect the Raman spectrum of sanidine. In other words, a shock pressure below 14 GPa will cause only minimal crystal structure change. Moderately shocked feldspar was subjected to shock pressure of more than 30 GPa. Under such pressure, although original twin lamellae are still preserved in part of feldspar grain, only weak peaks were shown at 479, 507 and 1114 cm^{-1} (Figure 3), indicating the crystal structure has become a more disordered crystal structure. This is consistent with the results of Kayama et al.'s [33] shock experiments of sanidine. Moreover, Fritz et al.'s [25] shock experiments on plagioclase also showed that, under a shock pressure of >30 GPa, only two broad humps could be identified at positions of about 500 and 980 cm^{-1}. Therefore, regardless of plagioclase or alkali feldspar, their crystal structures would be damaged under the shock pressure of >30 GPa and would even be transformed into glass.

4.4. Formation Process of Glass

Three kinds of glass were found in the Xiuyan crater in this study—diaplectic feldspar glass, VFG, and MMG—and they were from suevite. Suevite is a common impactite in impact craters and consists of various clasts of mineral, rock and melt with different shock features [34]. Therefore, although the three kinds of feldspar glass from the Xiuyan crater appear in the same breccia, they must have undergone different P-T histories. This also reflects the heterogeneity of shock pressure at different areas of the impact crater during the shock process [35].

Diaplectic albite glass is formed by solid-state transformation of mineral under high pressure without melting [36]. Thus, it seems that the post-shock temperature of moderately shocked feldspar does not exceed the liquidus temperature of albite. According to the shock classification system of felsic rocks by Stöffler et al. [11], diaplectic albite glass belongs to F-S5 stage, and its post-impact temperature is 300–900 °C, which does not exceed the liquidus temperature (1200 °C) of albite under ambient pressure [37]. Therefore, the diapectic albite glass was exposed to high pressure and a moderate temperature. According to Fritz et al. [25], diaplectic glass is the result of mechanical disaggregation of the crystal lattice into small domain sizes. In Figure 5d, the white arrow indicates a local shear trace, which may be related to the mechanical process.

VFG shows a lack of flow texture and has a clear boundary with the adjacent coesite-bearing silica glass, which indicates VFG does not mix with coesite-bearing silica glass. The occurrence indicates that the post-impact temperature is above the liquidus temperature at 1200 °C in albite [37,38] and below the liquidus temperature at 1600 °C in quartz [39]. We conclude that the VFG belongs to the F-S6 stage, and the post-shock temperature proposed by Stöffler et al. [11] is 900–1500 °C, which is consistent with this study. Chen et al. [14] estimated the duration of high pressure (>4.5 GPa) to be about 10 ms according to the size of coesite crystals in the silica glass. Therefore, VFG was exposed to high temperature and high pressure over a long time period as an impact event.

MMG with flow texture and schlieren indicates that the whole rock was melted during the shock process. Based on the chemical compositions of basement rocks from the Xiuyan crater [40], we conclude that the protolith of MMG is felsic rocks (gneiss or granulite). The felsic rocks from Xiuyan crater mainly consist of quartz and feldspar, as well as mica or amphibole, which is in line with the chemical compositions of MMGs in Table 1. The shock stage of MMG is F-S7, and the post-shock temperature is >1500 °C [11]. Moreover, due to high temperature after shock, the high-pressure phases are hard to preserve, so no high-pressure phase was found in the MMG.

5. Conclusions

The feldspars from the Xiuyan crater used for this study were alkali feldspar and had developed a variety of shock-metamorphic features, including irregular fractures, undulatory extinction, PDFs, diaplectic glass, and vesicular glass. The irregular factures and undulatory extinction developed in weakly shocked feldspar are classified as belonging to the F-S2 shock stage and indicate a shock pressure and post-shock temperature of ~5 to ~14 GPa and ~100 °C, respectively. PDFs and diaplectic glass coexist in moderately shocked feldspar, indicating a shock pressure and post-shock temperature of ~32 to ~45 GPa and 300–900 °C, respectively (F-S5 shock stage). Strongly shock feldspars occur as vesicular glass, which indicates a F-S6 shock stage involving a shock pressure and post-shock temperature of 45–60 GPa and 1200–1500 °C, respectively. MMG is the result of whole felsic rock melting, which indicates a shock pressure and post-shock temperature of >60 GPa and >1500 °C respectively (F-S7 shock stage).

Author Contributions: F.Y. developed and performed the experiments; F.Y. and D.D. analyzed the data; F.Y. wrote the paper. All authors have read and agreed to the published version of the manuscript.

Funding: This work was jointly funded by the National Natural Science Foundation of China (41503062, 41673070) and Natural Science Foundation of Hunan Province (2016JJ6039).

Acknowledgments: We thank Ming Chen for his constructive suggestions.

Conflicts of Interest: The authors declare no conflict of interest.

References

1. Nesse, W.D. *Introduction to Mineralogy*, 3rd ed.; Oxford University Press: Oxford, UK, 2017; pp. 249–255.
2. Rubin, A.E.; Ma, C. Meteoritic minerals and their origins. *Chem. Erde-Geochem.* **2017**, *77*, 325–385. [CrossRef]
3. Gucsik, A. Shock metamorphism at terrestrial impact structures: Mineralogical and geological consequences. *Acta Mineral. Petrol.* **2008**, *48*, 17–31.

4. Stöffler, D. Zones of impact metamorphism in the crystalline rocks of the Nördlinger Ries crater. *Contrib. Mineral. Petrol.* **1966**, *12*, 15–24. [CrossRef]
5. Pickersgill, A.E.; Osinski, G.R.; Flemming, R.L. Shock effects in plagioclase feldspar from the Mistastin Lake impact structure, Canada. *Meteorit. Planet. Sci.* **2015**, *50*, 1546–1561. [CrossRef]
6. Kovach, H.; Jones, R. Feldspar in type 4–6 ordinary chondrites: Metamorphic processing on the H and LL chondrite parent bodies. *Meteorit. Planet. Sci.* **2010**, *45*, 246–264. [CrossRef]
7. Yin, F.; Liao, Z.; Hursthouse, A.; Dai, D. Shock-induced olivine-ringwoodite transformation in the shock vein of chondrite GRV053584. *Minerals* **2018**, *8*, 139. [CrossRef]
8. Pang, R.-L.; Zhang, A.-C.; Wang, S.-Z.; Wang, R.-C.; Yurimoto, H. High-pressure minerals in eucrite suggest a small source crater on Vesta. *Sci. Rep.* **2016**, *6*, 26063. [CrossRef]
9. Greshake, A.; Schmitt, R.; Stöffler, D.; Pätsch, M.; Schultz, L. Dhofar 081: A new lunar highland meteorite. *Meteorit. Planet. Sci.* **2001**, *36*, 459–470. [CrossRef]
10. Sharp, T.G.; Walton, E.L.; Hu, J.; Agee, C. Shock conditions recorded in NWA 8159 Martian augite basalt with implications for the impact cratering history on Mars. *Geochim. Cosmochim. Acta* **2019**, *246*, 197–212. [CrossRef]
11. Stöffler, D.; Hamann, C.; Metzler, K. Shock metamorphism of planetary silicate rocks and sediments: Proposal for an updated classification system. *Meteorit. Planet. Sci.* **2018**, *53*, 5–49. [CrossRef]
12. Jaret, S.J.; Kah, L.C.; Harris, R.S. Progressive deformation of feldspar recording low-barometry impact processes, Tenoumer impact structure, Mauritania. *Meteorit. Planet. Sci.* **2014**, *49*, 1007–1022. [CrossRef]
13. Von Engelhardt, W.; Stöffler, D. Stages of shock metamorphism in crystalline rocks of the Ries basin, Germany. In *Shock Metamorphism of Natural Materials*; French, B.M., Short, N.M., Eds.; Mono Book Corp.: Baltimore, MD, USA, 1968; pp. 159–168.
14. Chen, M.; Xiao, W.; Xie, X. Coesite and quartz characteristic of crystallization from shock-produced silica melt in the Xiuyan crater. *Earth Planet. Sci. Lett.* **2010**, *297*, 306–314. [CrossRef]
15. Gillet, P.; Chen, M.; Dubrovinsky, L.S.; Goresy, A.E. Natural $NaAlSi_3O_8$-hollandite in the shocked Sixiangkou meteorite. *Science* **2000**, *287*, 1633–1636. [CrossRef] [PubMed]
16. Miyahara, M.; Ohtani, E.; Yamaguchi, A. Albite dissociation reaction in the Northwest Africa 8275 shocked LL chondrite and implications for its impact history. *Geochim. Cosmochim. Acta* **2017**, *217*, 320–333. [CrossRef]
17. Chen, M.; Xiao, W.S.; Xie, X.D.; Tan, D.Y.; Cao, Y.B. Xiuyan crater, China: Impact origin confirmed. *Chin. Sci. Bull.* **2010**, *55*, 1777–1781. [CrossRef]
18. Chen, M.; Yin, F.; Li, X.D.; Xie, X.D.; Xiao, W.S.; Tan, D.Y. Natural occurrence of reidite in the Xiuyan crater of China. *Meteorit. Planet. Sci.* **2013**, *48*, 796–805. [CrossRef]
19. Chen, M.; Gu, X.; Xie, X.; Yin, F. High-pressure polymorph of TiO_2-II from the Xiuyan crater of China. *Chin. Sci. Bull.* **2013**, *58*, 4655–4662. [CrossRef]
20. Chen, M.; Shu, J.; Xie, X.; Tan, D.; Mao, H.K. Natural diamond formation by self-redox of ferromagnesian carbonate. *Proc. Natl. Acad. Sci. USA* **2018**, *115*, 2676–2680. [CrossRef]
21. Chen, M.; Shu, J.; Xie, X.; Tan, D. Maohokite, a post-spinel polymorph of $MgFe_2O_4$ in shocked gneiss from the Xiuyan crater in China. *Meteorit. Planet. Sci.* **2019**, *54*, 495–502. [CrossRef]
22. Kieffer, S.W. Shock metamorphism of the coconino sandstone at Meteor crater, Arizona. *J. Geophys. Res.* **1971**, *76*, 5449–5473. [CrossRef]
23. Sharp, T.G.; DeCarli, P.S. Shock effects in meteorites. In *Meteorites and the Early Solar System II*; Lauretta, D.S., McSween, H.Y., Eds.; University of Arizona Press: Tucson, AZ, USA, 2006; pp. 653–677.
24. Jaret, S.J.; Johnson, J.R.; Sims, M.; DiFrancesco, N.; Glotch, T.D. Microspectroscopic and petrographic comparison of experimentally shocked albite, andesine, and bytownite. *J. Geophys. Res. Planets* **2018**, *123*, 1701–1722. [CrossRef]
25. Fritz, J.; Assis Fernandes, V.; Greshake, A.; Holzwarth, A.; Böttger, U. On the formation of diaplectic glass: Shock and thermal experiments with plagioclase of different chemical compositions. *Meteorit. Planet. Sci.* **2019**, *54*, 1533–1547. [CrossRef]
26. Sims, M.; Jaret, S.J.; Carl, E.-R.; Rhymer, B.; Schrodt, N.; Mohrholz, V.; Smith, J.; Konopkova, Z.; Liermann, H.-P.; Glotch, T.D. Pressure-induced amorphization in plagioclase feldspars: A time-resolved powder diffraction study during rapid compression. *Earth Planet. Sci. Lett.* **2019**, *507*, 166–174. [CrossRef]
27. Rubin, A.E. Maskelynite in asteroidal, lunar and planetary basaltic meteorites: An indicator of shock pressure during impact ejection from their parent bodies. *Icarus* **2015**, *257*, 221–229. [CrossRef]

28. Tschermak, G. *Die Meteoriten von Shergotty und Gopalpur*; KK Hof-und Staatsdruckerei: Wien, Austria, 1872.
29. Chen, M.; El Goresy, A. The nature of maskelynite in shocked meteorites: Not diaplectic glass but a glass quenched from shock-induced dense melt at high pressures. *Earth Planet. Sci. Lett.* **2000**, *179*, 489–502. [CrossRef]
30. Gibson, R.L.; Reimold, W.U. Shock pressure distribution in the Vredefort impact structure, South Africa. *Geol. Soc. Am. Special Paper* **2005**, *384*, 329–349.
31. Velde, B.; Boyer, H. Raman microprobe spectra of naturally shocked microcline feldspars. *J. Geophys. Res. Planets* **1985**, *90*, 3675–3682. [CrossRef]
32. Fritz, J.; Greshake, A.; Stöffler, D. Micro-Raman spectroscopy of plagioclase and maskelynite in Martian meteorites: Evidence of progressive shock metamorphism. *Antarct. Meteorit. Res.* **2005**, *18*, 96–116.
33. Kayama, M.; Nishido, H.; Sekine, T.; Nakazato, T.; Gucsik, A.; Ninagawa, K. Shock barometer using cathodoluminescence of alkali feldspar. *J. Geophys. Res. Planets* **2012**, *117*. [CrossRef]
34. Stöffler, D.; Grieve, R.A.F. Impactites, Chapter 2.11. In *Metamorphic Rocks: A Classification and Glossary of Terms, Recommendations of the International Union of Geological Sciences Subcommission on the Systematics of Metamorphic Rocks*; Fettes, D., Desmons, J., Eds.; Cambridge University Press: Cambridge, UK, 2007; pp. 82–92.
35. French, B.M. *Traces of Catastrophe: A Handbook of Shock-Metamorphic Effects in Terrestrial Meteorite Impact Structures*; Lunar and Planetary Institute: Houston, TX, USA, 1998.
36. Langenhorst, F.; Deutsch, A. Shock metamorphism of minerals. *Elements* **2012**, *8*, 31–36. [CrossRef]
37. Birch, F.; LeCompte, P. Temperature-pressure plane for albite composition. *Am. J. Sci.* **1960**, *258*, 209–217. [CrossRef]
38. Boyd, F.R.; England, J.L. Effect of pressure on the melting of diopside, $CaMgSi_2O_6$, and albite, $NaAlSi_3O_8$, in the range up to 50 kilobars. *J. Geophys. Res.* **1963**, *68*, 311–323. [CrossRef]
39. Zhang, J.; Li, B.; Utsumi, W.; Liebermann, R.C. In situ X-ray observations of the coesite-stishovite transition: Reversed phase boundary and kinetics. *Phys. Chem. Miner.* **1996**, *23*, 1–10. [CrossRef]
40. Yin, F. *Characteristics and Shock Effects of Impact Breccias from the Xiuyan Impact Crater*; University of Chinese Academy of Sciences: Beijing, China, 2014.

© 2020 by the authors. Licensee MDPI, Basel, Switzerland. This article is an open access article distributed under the terms and conditions of the Creative Commons Attribution (CC BY) license (http://creativecommons.org/licenses/by/4.0/).